UCRL-MI-140345

Recent Results in the Development of Fast Neutron Imaging Techniques

J. Hall, F. Dietrich, C. Logan, B. Rusnak

September 11, 2000

U.S. Department of Energy

Lawrence
Livermore
National
Laboratory

DISCLAIMER

This work was performed under the auspices of the U. S. Department of Energy by the University of California, Lawrence Livermore National Laboratory under Contract No. W-7405-Eng-48.

Recent Results in the Development of Fast Neutron Imaging Techniques

James Hall, Frank Dietrich, Clint Logan and Brian Rusnak

Lawrence Livermore National Laboratory
P.O. Box 808, M/S L-050, Livermore, CA 94551-9900

We are continuing with the development of fast (≈ 12 MeV) neutron imaging techniques for use in NDE applications. Our goal is to develop a neutron imaging system capable of detecting sub-mm-scale cracks, cubic-mm-scale voids and other structural defects in heavily-shielded low-Z materials within thick sealed objects. The final system will be relatively compact (suitable for use in a small laboratory) and capable of acquiring both radiographic and full tomographic image sets. The design of a prototype imaging detector will be reviewed and results from several recent imaging experiments will be presented. The concurrent development of an intense, accelerator-driven neutron source suitable for use with the final production imaging system will also be discussed.

INTRODUCTION

We are continuing with the development of fast neutron imaging techniques to complement (*not* replace) existing photon imaging techniques in NDE applications involving the inspection of thick sealed objects ($\rho x \gtrsim 100$ g/cm^2). Our goal is to develop a high-energy neutron imaging system capable of detecting sub-mm-scale cracks, cubic-mm-scale voids and other structural defects in heavily-shielded low-Z materials within such objects. The final production system will be relatively compact (suitable for use in a small laboratory) and capable of acquiring both radiographic and full tomographic image sets. In order to expedite the development process and minimize associated technical risks, we are using commercially-available system components and proven neutron imaging techniques wherever possible. As currently envisioned, the final production system will consist of an intense, accelerator-driven D(d,n)^{3}He neutron source ($E_n \approx 12$ MeV @ 0°) with an effective yield of $\approx 8.5 \times 10^{10}$ n/sec/sr along the beam axis and an effective spot size ≈ 1.25 mm (FWHM), a multi-axis staging system to support and manipulate objects under inspection and an imaging detector (*cf.* Figure 1). The imaging detector itself will consist of a plastic scintillator viewed indirectly by a cryogenically-cooled, high-resolution (2048 X 2048; 24 µm pixel) CCD camera. The ultimate spatial resolution of the system should be ≈ 0.50 – 1.00 mm (FWHM) at the object position.

The conceptual design of our imaging system (1, 2) and the results of early imaging experiments (3) have already been published elsewhere. In this paper, we will review the design of a prototype imaging detector and present results from several recent imaging experiments. The parallel development of an intense neutron source will also be discussed.

IMAGING DETECTOR DESIGN

The design of the imaging detector proposed for use in our system is derived from proven U.S. Nuclear Test Program technology. Our prototype for the detector consists of a rigid plastic scintillator viewed indirectly by a single CCD camera. The camera assembly consists of a fast (f/1.00; 50 mm) photographic lens coupled through a remotely-controlled mechanical shutter housing to a thinned, back-illuminated, high-resolution (1024 X 1024; 24 µm pixel) CCD imaging chip with an anti-reflective (UVAR) coating on its active area to improve its sensitivity to light from the scintillator. The chip is cryogenically cooled and operated at a controller-stabilized temperature of -120 °C which effectively eliminates thermal electronic noise buildup in the pixel wells. This allows for extended image integration times (≈ 1 hr) and greatly enhances the sensitivity of the camera in low light situations. Data is downloaded to the camera controller using a 16-bit A/D converter running at 50 kHz which imposes an average read-out noise on the image of ≈ 5 electrons/pixel. When compared to the full well capacity of the CCD chip (≈ 325,000 electrons/pixel), this gives an effective dynamic range for the camera in excess of ≈ 50,000 (a broad dynamic range is essential in tomographic imaging problems involving extremely thick objects since the camera must be able to resolve subtle intensity variations in the "shadowed" portion of an image without saturating in adjacent "open field" segments). A thin (0.125"), front-surfaced mirror fabricated from aluminized Pyrex glass is used to reflect light from the 30 cm X 30 cm X 4 cm-thick BC-400 plastic scintillator into the camera assembly which is mounted on dual-axis optical rails adjacent to the neutron beam path. The entire detector assembly is housed in a light-tight plywood enclosure with thin (0.125") aluminum entrance and exit apertures for the neutron beam.

RECENT IMAGING EXPERIMENTS

Experimental setup

In the experiments described here, a nearly monoenergetic, 10-MeV neutron beam was generated by focussing 6.85-MeV D^+ ions extracted from the Ohio University Accelerator Laboratory (OUAL) tandem van de Graaff accelerator into a cylindrical, 1-cm-diameter, 7.5-cm-long D_2 gas cell attached to the end of a beam line. The gas cell was capped with thin (≈ 5 μm) W entrance and exit windows and maintained at a static pressure of ≈ 45 psia (≈ 3.1 atm). Average D^+ ion currents measured at the gas cell were ≈ 8 μA during the runs and the diameter of the beam focal spot at the entrance window to the cell was ≈ 3.5 mm. This provided an effective neutron yield of ≈ $4.2x10^9$ n/sec/sr along the beam axis (*i.e.* ≈ 1/20th the intensity of the source proposed for our final production imaging system).

The objects imaged in the experiments were mounted on a multi-axis staging system which was located on the beam axis ≈ 2 m downstream from the neutron source. The prototype imaging detector was located in a shielded detector cave ≈ 2 m further downstream behind a thick (≈ 1.5 m) concrete with a tapered polyethylene collimator. This provided a 2:1 image magnification factor with a clear field-of-view (FOV) ≈ 12" in diameter at the detector position (FOV diameter ≈ 6" at the object position). While essentially a mater of convenience at OUAL, both analytical calculations and detailed Monte Carlo simulations have shown that a 2:1 magnification factor also minimizes radiation backgrounds at the image plane associated with "internal" scattering within the object (internal scattering can present a problem when imaging thick objects with curved contours since particles scattered near the limb suffer very little attenuation before leaving the object).

Imaging results

A series of seven neutron imaging experiments have thus far been carried out at OUAL. These experiments focussed on radiographic (single view) imaging of conventional step wedges made of various materials and "slab" assemblies composed of blocks of low-Z materials (*e.g.* polyethylene).shielded by various thicknesses (≤ 4") of Pb or depleted uranium (D-38) and tomographic (multiple view) imaging of cylindrical test objects composed of nested shells of high- and low-Z materials (see (3) for details). In this paper we present recent radiographic imaging data on fractured ceramics shielded by D-38 and "mock" tomographic reconstructions of the British Test Object.

The ceramic/poly/D-38 test object consisted of a 4" X 2" X 1"-thick slab of borated-ceramic set atop a polyethylene slab of similar size and shielded by 1" of D-38 (areal density ≈ 50.2 g/cm^2). The ceramic piece featured two sets of 4- and 2-mm-diameter holes machined to depths of 0.160", 0.120", 0.080" and 0.040" (the smallest hole corresponds to a volume defect of ≈ 3 mm^3 and an areal density defect of ≈ 0.20 g/cm^2) and a narrow slot cut down from the top to a depth of 1" (*cf.* Figure 2a). This slot was used to facilitate cracking the ceramic along its centerline. The poly piece featured the same set of 4- and 2-mm-diameter holes but no crack. The ceramic was carefully reassembled with the fracture being barely visible to the naked eye and the shielded assembly was imaged in a series of 48 30 minute exposures (time integrated flux at object position ≈ $1.1x10^{10}$ n/cm^2) with each image yielding ≈ 1400 counts/pixel above the CCD camera's built-in DC offset level. The final processed image and associated lineouts (*cf.* Figure 2b) clearly show the crack in the ceramic slab and all of the machined features including even the smallest, 2-mm-diameter, 0.040"-deep hole.

The British Test Object ("BTO"), on loan to the Department of Energy from AWE, Aldermaston for the express purpose of evaluating the performance of proposed NDE systems, consisted of a set of six nested cylindrical shells of (respectively) graphite, polyethylene, Al, W, polyethylene and W with a solid polyethylene core (*cf.* Figure 3a). The cylindrical shells were each segmented to provide an axially-symmetric joint structure. The full assembly had an OD of 18.9 cm and its areal density ranged from 125.93 g/cm^2 (along the centerline) to 176.40 g/cm^2 (along the limb of the poly core). Since the diameter of the BTO was somewhat too large to fit into our restricted FOV at OUAL, only a portion (≈ 60%) of the object was imaged. A series of 12 30 minute exposures (time integrated flux at object position ≈ $2.4x10^9$ n/cm^2) were taken of the assembly and, since it was axially symmetric, only a single viewing angle was used. The final processed image was then cropped at the center of the object and reflected about that line to produce an artificial image of the full assembly. This was then replicated 180 times to produce a "mock" tomographic data set. Subsequent reconstructions done using LLNL's Constrained Conjugate Gradient (CCG) algorithm (*cf.* Figure 3b) clearly show the gross structure of the BTO and also reveal the detailed joint structure in the outer shells. Note that, in spite of the fact that the tomographic data set used for reconstruction was derived in a somewhat artificial way, it *does* still provide an accurate demonstration of the capability of neutron imaging even when relatively short exposures are used (comparing the neutron flux available at OUAL during this run to that anticipated using our final, full-scale system, the time required to produce this image would have been ≈ 25 minutes).

NEUTRON SOURCE DEVELOPMENT

The development of an intense, high-energy neutron source suitable for use in a full-scale imaging system is proceeding in parallel with our work on the prototype detector and staging system. As noted above, we propose to use an accelerator-driven $D(d,n)^3He$ neutron source operating at ≈ 12 MeV. In order to meet our performance goals, the source will need to have an effective yield of ≈ 8.5×10^{10} n/sec/sr along the beam axis and an effective spot size ≈ 1.25 mm (FWHM). A high-energy DD neutron source is preferred here over a more conventional DT source because it provides natural (kinematic) collimation of the neutron beam which minimizes "external" scattering from walls, floors, etc. and thereby reduces radiation shielding requirements. The most promising system (and our likely choice) is a compact radio-frequency quadruplole (RFQ) accelerator coupled to a drift-tube linac (DTL) (4). The accelerator system will need to deliver an average D^+ ion current ≈ 300 μA at the gas cell in order to produce a neutron flux sufficient to image objects of interest. While this is certainly achievable with current technology, it does pose another, in some ways more challenging, problem: the combined requirements of a high D^+ ion current and small focal spot size effectively preclude the use of conventional ("windowed") D_2 gas cell designs due to their inability to handle the large heat loads involved (≈ 250 kW/cm^2 (ave)). A more innovative approach is required.

We are collaborating with R. Lanza at the Massachusetts Institute of Technology (MIT) on the development of two types of "windowless" D_2 gas target assemblies which could be coupled to a high-current D^+ accelerator and used as a neutron source. The first consists of a high-pressure (≈ 2 - 3 atm) D_2 gas cell mounted at the exit port of a differentially-pumped chamber with three stages isolated from one another by a series of rotors with apertures synchronized to the pulse frequency of the accelerator. A windowless target of this type minimizes energy loss in the D^+ beam and is particularly well suited for use with accelerator systems such as RFQ linacs which tend to operate with very high peak ion currents and relatively low duty factors. Operational testing of a prototype "rotating aperture" target is currently underway at MIT (5).

An alternative to the rotating aperture target is also being investigated at MIT. The basic technique involves the use of an intense, axial plasma discharge to effectively "plug" the aperture of a high-pressure gas cell by rapidly heating and ionizing gas leaking down the exit channel (*cf.* Figure 4). This increases the viscosity of the gas in the channel and creates a region of high pressure (but low density) which balances the pressure in the cell and yet remains transparent to charged particle beams. This type of target offers several advantages over the "rotating aperture" design. First (and most obvious), it has no moving parts and is thus easier to assemble and maintain. Second, it operates in a "steady-state" mode which allows for the use of effectively CW beams and reduces the thermodynamic stress on the gas in the cell. Finally, it has a favorable focusing effect on charged particle beams. In recent tests at MIT using a regulated Ar gas cell, a prototype "plasma window" target was able to sustain a pressure differential in excess of 2.5 atm across a small (≈ 3 mm) aperture with an upstream pressure of ≈ 10^{-6} torr (6). This type of target is our current preference (with the rotating aperture design held in reserve) and we are continuing to work with MIT to refine its design and assess its operational capability and lifetime.

CONCLUSIONS

The experiments carried out thus far have demonstrated the essential feasibility of using high-energy neutron imaging as a complement to existing photon imaging techniques in applications involving the inspection of thick sealed objects and we are poised to commit to the construction of a full-scale facility. Additional tests of the prototype imaging detector are planned at OUAL (focussed primarily on certifying the capabilities of neutron imaging, improving the efficiency of the detector and evaluating alternate scintillator materials) and key decisions on target and accelerator technologies will be made during early 2001. We have already identified vendors of optical imaging systems and small accelerator systems which might be suitable for use in a full-scale neutron imaging system and are currently finalizing performance specifications. In addition, design drawings for a full-scale multi-axis staging system rated for NDE have recently been obtained from the DOE plant at Y-12 in Oak Ridge, TN and we are ready to proceed with the fabrication of that system.

ACKNOWLEDGMENTS

We would like to thank Prof. David Ingram of Ohio University and the staff of OUAL for their continued support in the testing of our prototype imaging detector and Jessie Jackson and Dr. Harry Martz of LLNL for their assistance in tomographic image reconstructions. Finally, we would like to thank Prof. Richard Lanza of MIT and his students for their support in the ongoing development of the high-yield neutron source.

This work was performed at the University of California, Lawrence Livermore National Laboratory, under the auspices of the U.S. Department of Energy (contract # W-7405-Eng-48).

REFERENCES

1. F. Dietrich and J. Hall, "Detector concept for neutron tomography in the 10 - 15 MeV energy range", LLNL report # UCRL-ID-123490, 4 pp. (1996).
2. F. Dietrich, J. Hall and C. Logan, "Conceptual design for a neutron imaging system for thick target analysis operating in the 10 - 15 MeV energy range," published in J. Duggan and I. Morgan (eds.), *Application of Accelerators in Research and Industry* (AIP **CP392**), New York, NY: AIP Press, 1997, p. 837-840.
3. J. Hall, F. Dietrich, C. Logan and G Schmid, "Development of high-energy neutron imaging for use in NDE applications", SPIE **3769**, 31-42 (1999) (UCRL-JC-134562); abridged version also published in AIP **CP497**, 693-698 (1999).
4. B. Rusnak and J. Hall, "An accelerator system for neutron radiography," published in these proceedings.
5. E. Empey, Master's thesis (unpublished), Massachusetts Institute of Technology, Cambridge, MA, January 2000.
6. W. Gerber, R. Lanza, A. Hershcovitch, P. Stephan, C. Castle and E. Johnson, "The plasma porthole: a windowless vacuum-pressure interface with various accelerator applications," published in J. Duggan and I. Morgan (eds.), *Application of Accelerators in Research and Industry* (AIP **CP475**), New York, NY: AIP Press, 1999, p. 932-935.

COLLECTED FIGURES

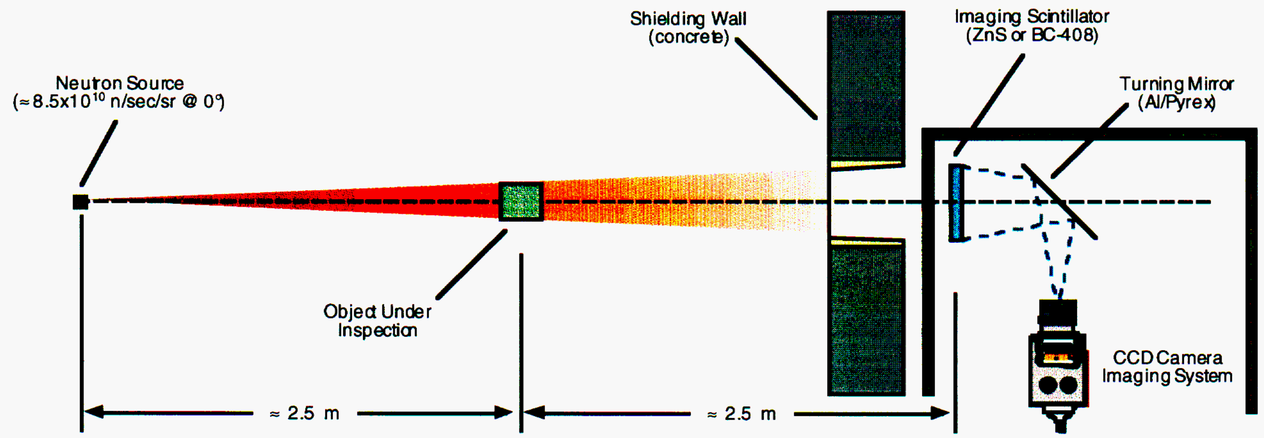

Figure 1: Conceptual schematic of proposed high-energy neutron imaging system. Using a 2:1 image magnification factor minimizes backgrounds at the imaging plane caused by internal scattering within the object under inspection.

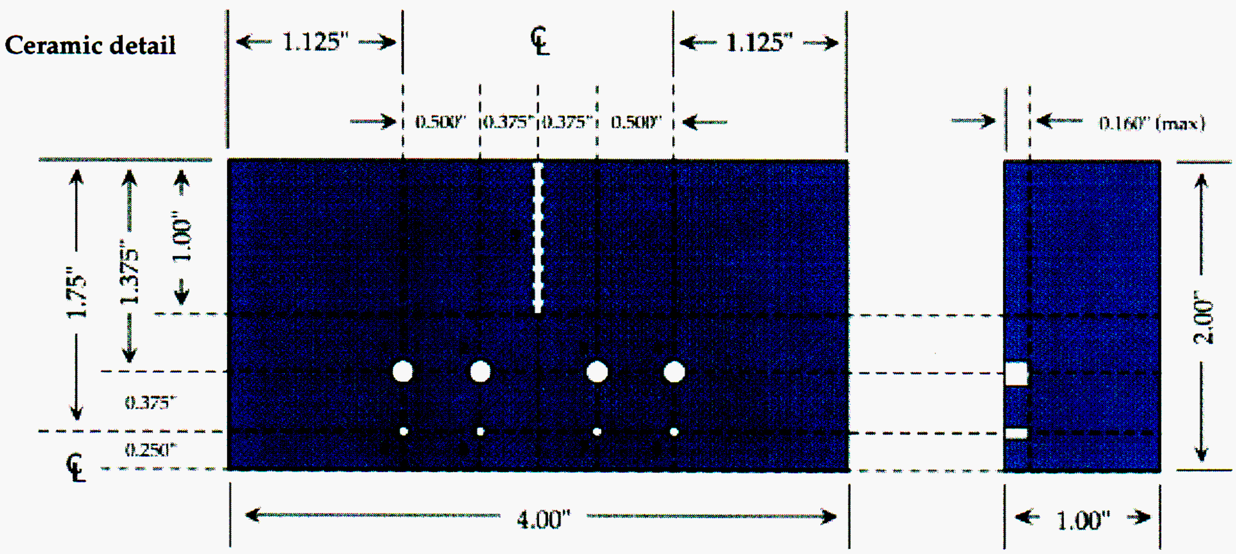

Feature dimensions -

1: 4 mm Ø, 0.120" deep (flat bottom)

2: 4 mm Ø, 0.040" deep (flat bottom)

3: 4 mm Ø, 0.080" deep (flat bottom)

4: 4 mm Ø, 0.160" deep (flat bottom)

5: 2 mm Ø, 0.120" deep (flat bottom)

6: 2 mm Ø, 0.040" deep (flat bottom)

7: 2 mm Ø, 0.080" deep (flat bottom)

8: 2 mm Ø, 0.160" deep (flat bottom)

9: Slot or groove used to guide cracking

Figure 2a: Design drawing of ceramic test object featuring two parallel sets of 4- and 2-mm-diameter holes machined to depths of 0.160", 0.120", 0.080" and 0.040" (the smallest hole corresponds to a volume defect of ≈ 3 mm^3 and an areal density defect of ≈ 0.20 g/cm^2) and a narrow slot cut down from the top to a depth of 1". This slot was used to facilitate cracking the ceramic along its centerline.

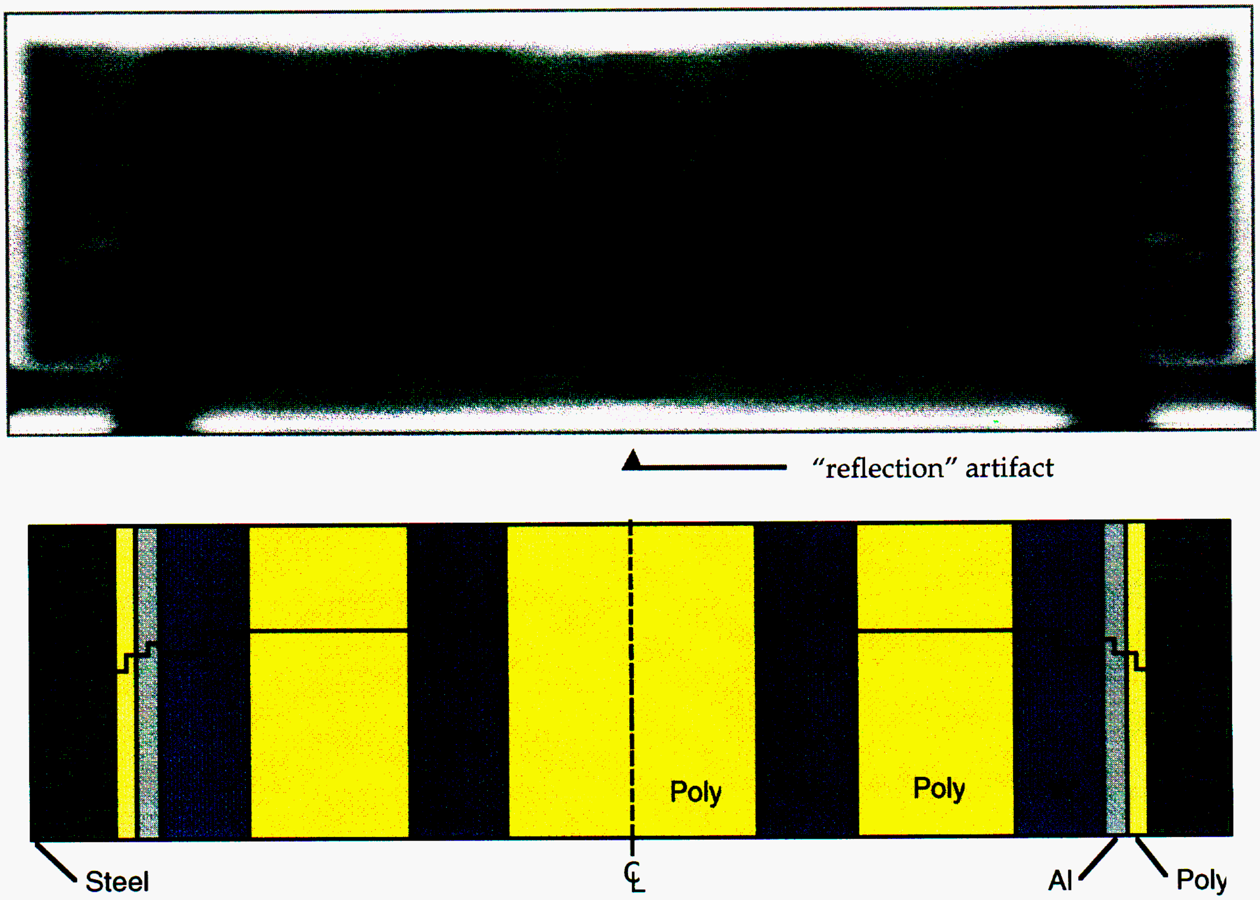

Figure 3b: "Mock" tomographic reconstruction of the BTO. The slice shown here was produced using a CCG reconstruction algorithm which takes the conical shape of the beam into account. Note that the gross structure of the BTO and the detailed joint structure in the outer shells is clearly visible in the reconstruction. The dark band at the center of the reconstruction is an artifact caused by reflecting the original radiograph about its centerline to form a complete image of the object.

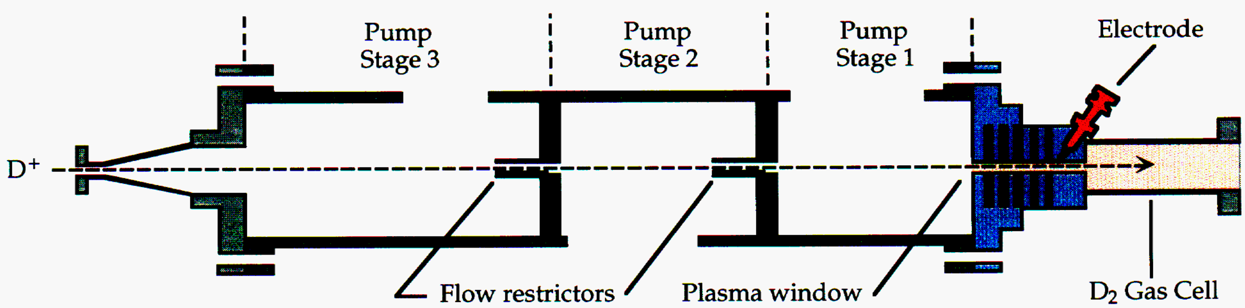

Figure 4: Generalized schematic of "plasma window" D_2 gas target design currently under development at MIT.

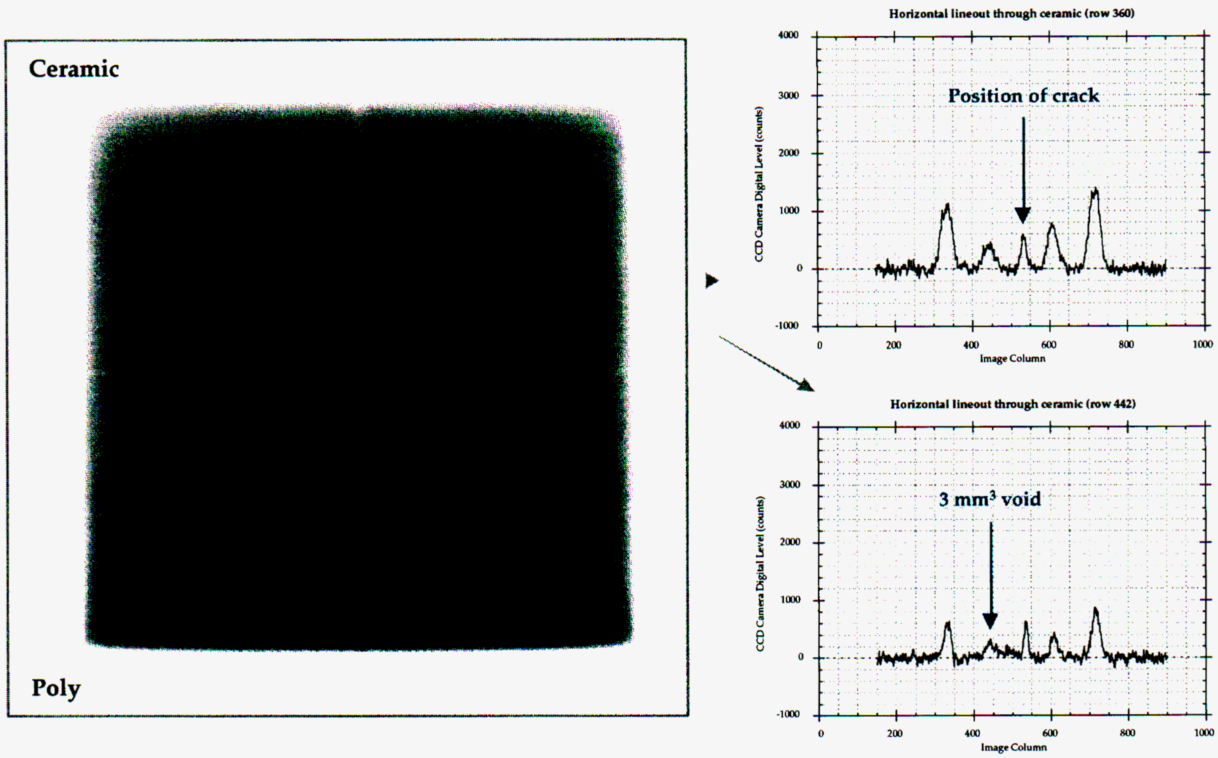

Figure 2b: Neutron radiograph of ceramic/poly/D-38 test object ($\rho x \approx 50.2\ g/cm^2$). The associated lineouts clearly show the crack in the ceramic slab and all of the machined features in both the ceramic and polyethylene.

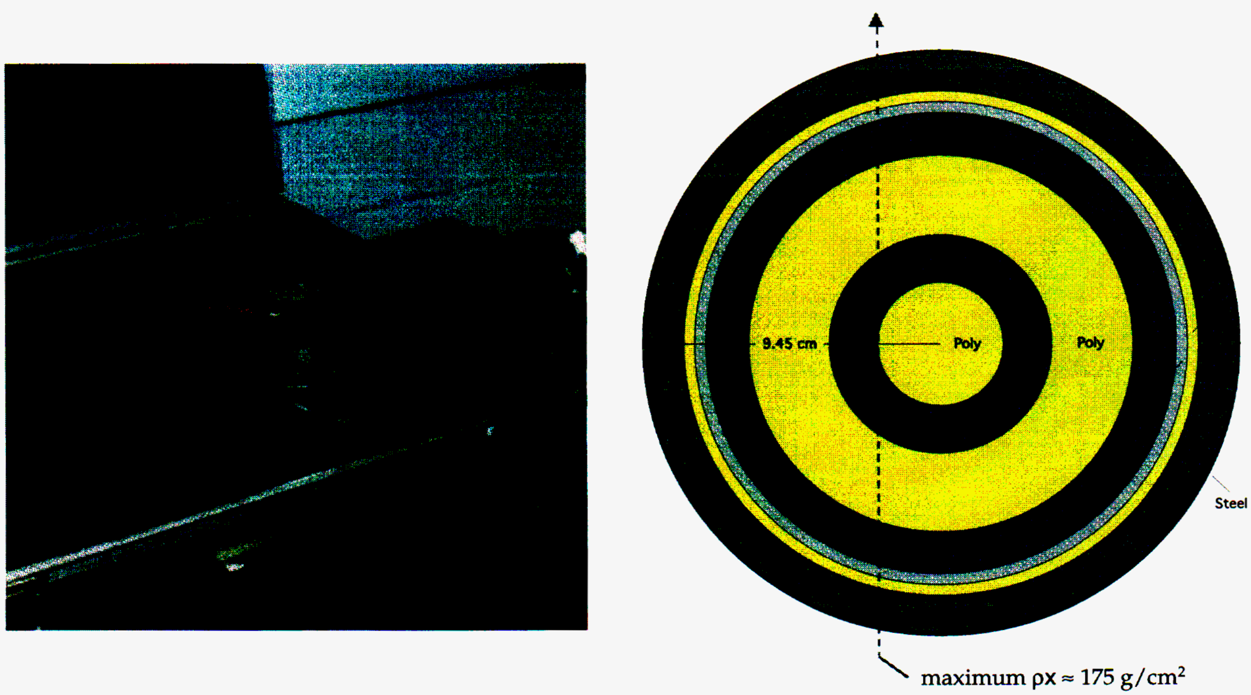

Figure 3a: Photograph and schematic drawing of the British Test Object (BTO) indicating structure and composition. The BTO is on loan to the DOE from AWE, Aldermaston for the express purpose of evaluating the performance of proposed NDE systems